Semi-Mechanistic Bayesian modeling of COVID-19 with Renewal Processes

Samir Bhatt[1], Neil Ferguson[1], Seth Flaxman[2], Axel Gandy[2,†], Swapnil Mishra[1], and James A. Scott[2]

[1]MRC Centre for Global Infectious Disease Analysis, Imperial College, London, UK
[2]Department of Mathematics, Imperial College, London, UK
[*]† Corresponding author: a.gandy@imperial.ac.uk

Abstract

We propose a general Bayesian approach to modeling epidemics such as COVID-19. The approach grew out of specific analyses conducted during the pandemic, in particular an analysis concerning the effects of non-pharmaceutical interventions (NPIs) in reducing COVID-19 transmission in 11 European countries. The model parameterizes the time varying reproduction number R_t through a regression framework in which covariates can e.g. be governmental interventions or changes in mobility patterns. This allows a joint fit across regions and partial pooling to share strength. This innovation was critical to our timely estimates of the impact of lockdown and other NPIs in the European epidemics, whose validity was borne out by the subsequent course of the epidemic. Our framework provides a fully generative model for latent infections and observations deriving from them, including deaths, cases, hospitalizations, ICU admissions and seroprevalence surveys. One issue surrounding our model's use during the COVID-19 pandemic is the confounded nature of NPIs and mobility. We use our framework to explore this issue. We have open sourced an R package epidemia implementing our approach in Stan. Versions of the model are used by New York State, Tennessee and Scotland to estimate the current situation and make policy decisions.

1 Introduction

This article presents a general framework for semi-mechanistic Bayesian modeling of infectious diseases using renewal processes. The term semi-mechanistic relates to statistical estimation within some constrained mechanism. Variants of this general model have been used in specific analyses of Covid-19 (Flaxman et al., 2020b; Flaxman et al., 2020a; Vollmer et al., 2020; Mellan et al., 2020; Unwin et al., 2020; NYS Press Office, 2020; Olney et al., 2020; The Scottish Government, 2020; Mishra et al., 2020), and continue to be used in ongoing work to make policy decisions. These models should therefore be clearly motivated, their key statistical and epidemiological features understood, and limitations made clear. This article aims to fill this gap, motivating the framework through counting processes. Various extensions of the basic model are considered, including a latent infection process. We discuss limitations and applications of the modelling framework with this goal to stimulate further research.

The model uses a flexible regression-based framework for parameterising transmission and ascertainment rates. This allows us to fit multilevel models (Gelman and Hill, 2006; Hox, Moerbeek, and Schoot, 2010; Kreft and Leeuw, 2011) for several regions simultaneously. Such partial pooling of parameters has specific advantages in the context of infectious diseases. Suppose we wish to estimate the effect of NPIs (Cowling et al., 2020; Flaxman et al., 2020b) or mobility (Badr et al., 2020; Miller et al., 2020) on transmission rates. Estimating this effect separately in different regions could lead to noisy estimates for at least two reasons. There is typically little high quality data at the early stages of an epidemic. Such data is generally correlated, reducing the information content that can be used to infer such an effect. In addition, NPIs often occur in quick succession and their effects are confounded (HKSAR, 2003; WHO, 2003). This is exacerbated by the random time between infections (the generation distribution) and the lag between infections and observations. This smooths the observed data, making it more difficult to attribute changes in transmission rates to a particular NPI. Alternatively, one could pool the effect across all groups. This ignores group-level variations and can lead to poor predictive performance, in particular underestimating variance for previously unmodeled regions. One could augment such a model with group-level indicators, but this results in a large number of parameters, which are difficult to estimate and leads to overfitting with classical estimation techniques. Partial pooling provides a natural solution to this.

Sometimes the inferential goal is not to assess the effect of a covariate on outcomes, but rather to infer transmission rates over time. Previous studies have focused on estimating reproduction numbers from case data (Ferguson, Donnelly, and Anderson, 2001; Riley et al., 2003; Bettencourt and Ribeiro, 2008; Fraser et al., 2009; Kelly et al., 2010; Cori et al., 2013), sometimes directly substituting observed case counts for the unknown number of infected individuals (Wallinga and Teunis, 2004). However, the emergence of SARS-CoV-2 has highlighted shortcomings of methods that rely on just case data. Limited testing capacity at the early stages of the pandemic led to only a small proportion of infections being detected and reported (Li et al., 2020). Those tested were typically more likely to have been hospitalised or were at higher risk of infection or death. In particular this proportion, referred to as the infection ascertainment rate (IAR) is country-specific and likely to have changed over time due to changes in testing policies and capacity. If unaccounted for, it will lead to biases in the inferred transmission rates.

This highlights the need for more flexible observational models, whereby more varied types of data can be incorporated, and their idiosyncrasies accounted for. Daily death data has been used in Flaxman et al. (2020b) to recover reproduction numbers in the early stages of the SARS-CoV-2 pandemic, and has been seen as more reliable than case data. However, there have been clear variations in definitions and reporting across time and countries. It is therefore important to appropriately model noise within the the observational models. Our framework allows for multiple types of data including deaths, cases, hospitalizations, ICU admissions and the results of seroprevalence surveys. This improves robustness of inferred parameters to biases in any one type of data.

The model uses discrete renewal processes to propagate infections within modeled populations. These have been used in a number of previous studies (Fraser, 2007; Cori et al., 2013; Nouvellet et al., 2018; Cauchemez et al., 2008), and are linked to other popular approaches to infectious disease modeling. Champredon, Dushoff, and Earn (2018) show that the renewal equation leads to identical dynamics as Erlang-Distributed Susceptible-Exposed-Infected-Recovered (SEIR) compartmental models, when a particular form is used for the generation distribution. A special case of this is the standard Susceptible-Infected-Recovered (SIR) model (Kermack, William Ogilvy and McKendrick, 1927). The approach is also connected to counting processes including the Hawkes process and the Bellman-Harris process (Bellman and Harris, 1948; Bellman and Harris, 1952). Bellman and Harris (1948) derive the renewal equation as the expectation of an age-dependent branching process. Age-dependence allows for more realistic dynamics than age-insensitive processes, like the Galton-Watson process (Bartoszynski, 1967; Getz and Lloyd-Smith, 2006). More complex branching processes such as the Crump-Mode-Jagers branching process could also be considered. Hawkes processes are also related to renewal processes, with the expectation of the Hawkes intensity function resulting in the renewal equation.

We describe the general model in detail, and start by considering the bare-bones version in Section 2. The motivation for the model lies in continuous-time counting processes, and this connection is discussed in Section 3. Sections 4 and 5 present the infection and observation processes in more detail, and consider important extensions of the basic model. Section 6 considers how to use the framework for multilevel modeling. Section 7 compares our approach to standard time series models, and outline the key challenges involved in modeling with our framework. Section 8 discusses two examples which consider the specific aspect of the confounding between interventions and observed data such as mobility data. Section 9 has a brief discussion.

2 Model Overview

We now formulate a basic version of the model for one homogeneous population. The same model can be used for multiple regions or groups jointly. Let $R_t > 0$ be the reproduction number at time $t > 0$. This determines the rate at which infections grow. Infections $i_v, \ldots, i_0$ for some $v \leq 0$ are given a prior distribution. For $t > 0$, we let new infections i_t be defined by

$$i_t = R_t \sum_{s<t} i_s g_{t-s}, \tag{1}$$

where g is a probability mass function for the generation time; defined as the lag between infections.

Observations occur at certain times $t > 0$. In general, there may be multiple types; case and death counts for example.

Each such type is driven by its own time-varying ascertainment rate $\alpha_t > 0$. The mean of the observations at time t is linked to past infections by

$$y_t = \alpha_t \sum_{s \leq t} i_s \pi_{t-s}, \tag{2}$$

where π is a distribution for the lag between an infection and when it gives rise to an observation. The sampling distribution of the distribution is typically nonegative and discrete, and may depend on auxiliary parameters. When multiple types are observed, we can superscript the quantities as $y_t^{(l)}, \alpha_t^{(l)}$ and $\pi^{(l)}$ and assign independent sampling distributions for each type.

Transmission rates R_t and ascertainment rates α_t can be modeled flexibly using Bayesian regression models, and through sharing of parameters, are the means through which we tie together multiple regions or groups using multilevel modeling. One can, for example, model transmission rates as depending on a binary covariate for an NPI, say full lockdown. The coefficient for this can be *partially pooled* between these groups. The effect is to share information between groups, while still permitting between group variation.

3 Motivation from continuous time

Our model can be motivated from a continuous time perspective as follows. Infections give rise to additional infections in the future, referred to as offspring. The timing and number of these offspring are determined by two objects, a probability distribution g on $\mathbb{R}^+$, and a non-negative stochastic process $\{R(t) : t > 0\}$. Suppose that g is continuous and admits a density. Letting $N^I(t)$ denote the number of infections occurring by time t, we define $N^I(t)$ for $t > 0$ by its intensity

$$\lambda(t) = R(t) \int_{s<t} g(t-s) N^I(ds). \tag{3}$$

The process can be initialised by assuming values for $N^I(t)$ for t in the seeding period $[v, 0]$. Equation (3) is similar to the Hawkes intensity, however the *memory kernel* g is scaled by a time-specific factor $R(t)$. The integrand g allows the intensity to increase due to previous infection events, while $R(t)$ tempers the intensity for other time-specific considerations. If $R(t') = R(t)$ for all t' then Equation (3) reduces to a Hawkes process. Under this assumption, since g integrates to unity, the expected number of offspring is simply $R(t)$, and so this is the *instantaneous reproduction number* or alternatively the *branching factor* of the Hawkes process. The generation time, defined as the time from an infection to a secondary infection, is distributed according to g and so g is the *generation distribution*.

Observations are precipitated by past infections; a given infection may lead to observation events in the future. Letting $N^Y(t)$ be the count of some observation type over time defined by the intensity

$$\lambda_y(t) = \alpha(t) \int_{s<t} \pi(t-s) N^I(ds), \tag{4}$$

for $t > 0$, where $\pi : \mathbb{R}^+ \to \mathbb{R}^+$ is a function and $\{\alpha(t) : t \geq 0\}$ is a non-negative stochastic process. This is similar to Equation (3), however the intensity increases due to past infections, rather than past observations. Suppose that π is a probability density, and let $\alpha(t') = \alpha(t)$ for all t'. The average number of observation events attributable to a single infection is then $\alpha(t)$, and so this is an *instantaneous ascertainment rate*. π is then interpreted as the distribution for the time from an infection to an observation, and is referred to as an *infection to observation* distribution.

4 Infection Process

The discrete formulation described in Section 2 is more amenable to inference. Here, we derive this model from the continuous counterpart. This helps to motivate some of the extensions discussed in subsequent sections. Let $I_t =$

$N_t^I - N_{t-1}^I$ be new infections at time t. The discrete version of Equation (3) is

$$\mathrm{E}[I_t|R_t, I_{v:t-1}] = R_t L_t, \tag{5}$$

where $L_t := \sum_{s<t} I_s g_{t-s}$ is the *case load* or total infectiousness by time $t > 0$. Moreover, taking the expected value of both sides given reproduction numbers and seeded infections results in

$$\begin{aligned} \mathrm{E}[I_t|R_{1:t}, I_{v:0}] &= R_t \, \mathrm{E}[L_t|R_{1:t}, I_{v:0}] \\ &= \sum_{s<t} \mathrm{E}[I_s|R_{1:s}, I_{v:0}] g_{t-s}. \end{aligned} \tag{6}$$

Defining $i_t := \mathrm{E}[I_t|R_{1:t}, I_{v:0}]$, we recognise this as Equation (1). This is a discrete renewal equation, which can alternatively be interpreted as an AR(t)-process with known coefficients g_k. From this point of view, the basic model in Section 2 uses i_t as synonymous with actual infections. Since infections are simply a deterministic function of other parameters, there is no need to treat them as unknown latent parameters to sample. This can lead to lower sampling times and faster convergence.

4.1 Modeling Latent Infections

The model of Section 2 can be extended by replacing each i_t with the actual infections from the counting process I_t, and then assigning a prior to I_t. Although sampling can be slower, this has certain advantages. When past infection counts are low, significant variance in the offspring distribution can imply that new infections I_t has high variance. This is not explicitly accounted for in the basic model. In addition, this approach cleanly separates infections and observations; the latter being modeled *conditional* on actual infections. The sampling distribution can then focus on idiosyncrasies relating to the observation process.

We assign a prior to I_t conditional on previous infections and current transmission R_t. The expected value for this is given by Equation (5). Appendix 10.1 shows that assuming the variance of the prior to be a constant proportion d of this mean is equivalent to letting d be the *coefficient of dispersion* for the offspring distribution. $d > 1$ implies overdispersion, and can be used to account for super-spreading events, which has been shown to be an important aspect for modeling Covid-19. The parameter d can be assigned a prior.

Any two parameter family can be used to match these first two moments. Letting this be continuous rather than discrete allows inference to proceed using Hamiltonian Monte Carlo, whereby new values for I_t are proposed simultaneously with all other parameters. Possible candidates include log-normal, gamma and the Weibull distributions. If an explicit distribution for the offspring distribution is desired, one can show that assuming a Gamma distribution with rate λ for this results in a Gamma distribution for I_t with rate λ. The coefficient of dispersion is then simply $D = \lambda^{-1}$.

4.2 Population Adjustments

If R_t remains above unity over time, infections grow exponentially without limit. In practice, infections should be bounded from above by S_0, the initial susceptible population. All else being equal, transmission rates are expected to fall as the susceptible population is diminished.

Consider first the model using I_t, which was described in Section 4.1. Equation 5 can be replaced with

$$\mathrm{E}[I_t|R_t, I_{v:t-1}] = (S_0 - I_{t-1}) \left(1 - \exp\left(-\frac{R_{u,t} L_t}{S_0}\right)\right), \tag{7}$$

where $R_{u,t}$ is an *unadjusted* reproduction number, which does not account for the susceptible population. This satisfies intuitive properties. As the *unadjusted* expected infections $R_{u,t} L_t$ approaches infinity, the *adjusted* expected value approaches the remaining susceptible population. The motivation for and derivation of Equation (7) is provided in Appendix 10.2. In short, this is the solution to a continuous time model whose intensity is a simplification of Equation (3). We must also ensure that the distribution of I_t cannot put positive mass above $S_0 - I_{t-1}$. A simple solution is to use truncated

distributions. Of course, this adjusts the mean value from Equation (7), however this is unlikely to be significant unless the susceptible population is close to depletion.

In the basic model, one can apply the adjustment to i_t by replacing L_t in Equation (7) with

$$\mathrm{E}(L_t|R_{1:t}, I_{v:0}) = \sum_{s<t} i_s g_{t-s}. \tag{8}$$

5 Observations

Observations are modeled in discrete time, analogous to how we treated infections in Section 4. Letting $\pi : \mathbb{N} \to \mathbb{R}^+$ and $Y_t := N_t^Y - N_{t-1}^Y$, the discrete analogue to Equation (4) is

$$\mathrm{E}[Y_t|\alpha_t, I_{v:t}] = \alpha_t \sum_{s \leq t} I_s \pi_{t-s}. \tag{9}$$

Taking the expected value of the above given seeded infections, transmission rates and the current ascertainment rate gives

$$\mathrm{E}[Y_t|\alpha_t, R_{1:t}, I_{v:0}] = \alpha_t \sum_{s \leq t} i_s \pi_{t-s}, \tag{10}$$

which is recognisable as Equation (2). Thus we have two possible expressions for the mean of Y_t, one given actual infections, and the other given expected infections i_t. The basic model of Section 2 uses the latter, while the extension in Section 4.1 uses the former.

We assume that $Y_t \sim \mathcal{F}(y_t, \phi)$, where $\mathcal{F}$ is a non-negative discrete family parameterised by its mean y_t and potentially an auxiliary parameter ϕ. This could be a Poisson distribution, where there is no auxiliary parameter. Using a quasi-Poisson or negative binomial instead allows for overdispersion. This can be useful to capture, for example, day-to-day variation in ascertainment rates when infection counts are low. The mean y_t can be taken to be either (9) or (10), the latter being used in the basic version of the model. Hidden in this formulation is the assumption that each Y_t is conditionally independent given y_t. Using multiple observation series $Y_t^{(l)}$ can help to improve the model inferences and identifiability of certain parameters. We simply assume that each such series is conditionally independent given the underlying infection process.

6 Multilevel Models

Transmission rates can be modeled quite generally within the framework. If the aim is simply to estimate transmission in a single region over time, one approach could be to let $R_t = g^{-1}(\gamma_t)$, where g is a link function and γ_t is some autocorrelation process, for example a random walk. Suppose, however, that transmission is modeled in M regions and the goal is to estimate the effect of a series of NPIs on transmission. Letting $R_t^{(m)}$ denote transmission in region m at time t, we could let

$$R_t^{(m)} = g^{-1}\left(\beta_0^{(m)} + \sum_{l=1}^{p} x_t^{(m)} \beta_k^{(m)}\right), \tag{11}$$

where $x_t^{(m)}$ are binary encodings of NPIs, and $\beta_0^{(m)}$ and $\beta_k^{(m)}$ are region-specific intercepts and effects respectively. The intercepts are used to allow regions to have their own baseline transmission rates. Collecting these group specific parameters into $\beta^{(m)}$, we can partially pool them by letting $\beta^{(m)} \sim \mathcal{N}(0, \Sigma)$, for each group m, and the assigning a prior to the covariance matrix Σ. This could be an inverse-Wishart prior, or alternatively, Σ can be decomposed into variances and a correlation matrix, which are each given separate priors (Tokuda et al., 2011).

One possible option for g is is the log-link. This provides easily interpretable effect sizes; a one unit change in a covariate multiplies transmission by a constant factor. However, this can lead to prior mass on unreasonably high

transmission rates. With this in mind, an alternative is to use a generalisation of the logit link for which

$$g^{-1}(x) = \frac{K}{1 + e^{-x}}, \tag{12}$$

and where K is the maximum possible value for transmission rates. This serves a similar purpose to the carrying capacity in a logistic growth model.

The ascertainment rate α_t can also be modeled with similar considerations to the above. This flexibility is useful, particularly because these quantities are likely to change as an epidemic progresses. This has been clearly seen during the Covid-19 epidemic, where the infection ascertainment rate may have increased over time due to increased testing capacity and improved track and trace systems. Multilevel models can in theory also be specified through α_t.

7 Forecasting, epidemiological constants, and seeding

A key benefit of using a semi-mechanistic approach is that forecasts are constrained by plausible epidemiological mechanisms. For example, in the absence of any further interventions or behavioural changes, and looking at a medium term forecast of just incidence (daily new cases/infections), a traditional time series forecasting approach may predict a constant function based on observing broadly constant incidence, but semi-mechanistic approach would expect a monotonic decrease based on a constant rate of transmission and the effect of herd immunity. The performance of epidemiologically constrained models is generally good; this is perhaps not surprising as examining the discrete renewal equation shows that these models correspond to autoregressive(n) filters with a convex combination of coefficients specified by the generation interval. However, similar to financial forecasting, the predictive capability of epidemic models are likely to be better interpreted as scenarios rather than actual predictions due to the rapidly adaptive landscape of policy.

A second benefit of epidemic models is to provide a plausible mechanism to explain (non causally) the changes observed in noisy data. For example, in estimating the effect of an intervention on observed death data, we need consider what that intervention affects i.e the rate of transmission or R_t. As we have described above, we can connect the rate of transmission to latent infections to deaths such that we have an epidemiologically motivated mechanism. While we can statistically estimate parameters for how the intervention affects R_t, certain important parameters will be entirely unidentifiable and need to be fixed as constants or with very tight priors. For example, to reliably estimate the number of infections, an infection fatality rate needs to be chosen. A failure to choose an appropriate infection fatality rate can result in a bimodal posterior where changes can either be attributed to herd immunity or to interventions. From a statistical perspective, is it difficult to disentanlge which mode of the posterior best represents reality, and hence it is sensible to first estimate a plausible infection fatality rate and then use this within the semi-mechanistic model. A second example is the onset of symptoms-to-death distribution. Given the lag between transmission, infection and deaths, the effect of an intervention is dependent on the onset of symptoms-to-death distribution.

Initially infection seeding is a fundamentally challenging aspect of epidemic modelling. Estimating the initial effect of seeding is crucial to understanding a baseline rate of growth (R_0) from which behaviours and interventions can modify. This seeding is heavily confounded by importation and under ascertainment. Both these factors can influence estimates of the initial growth rates, and this in turn can affect the impact of changes in transmission as time progresses. We have proposed heuristic approaches to mitigate issues with early seeing, but principled statistical approaches need to be developed. In particular, Bayesian pair plots show strong correlation between seeding parameters and R_0, which can potentially lead again to a bimodal posterior where initial growth dynamics can be explained through R_0 or via initial seed infections.

8 Examples

This section presents two example uses of the model. Both are modifications of the multilevel model in Flaxman et al. (2020b), which used daily death data to estimate the effect of NPIs in 11 European countries. Our first example demonstrates use of a simple two-stage alternative of this model. This approach separates the problem of estimating R_t

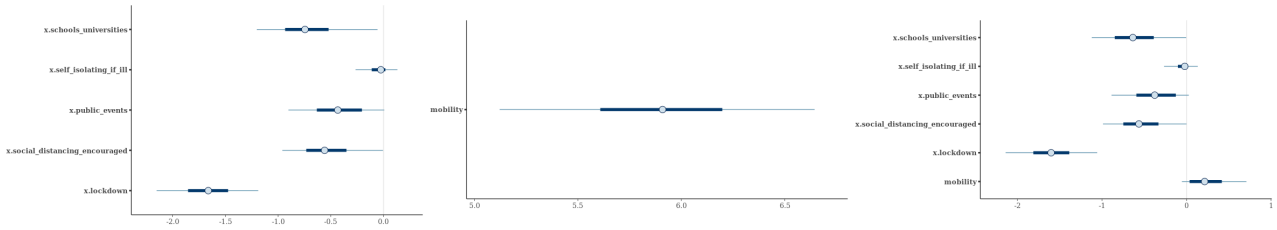

(a) (b) (c)

Figure 1: Regression of NPIs and/or mobility against nonparametric R_t. Figure (a) shows the fit for NPIs only. (b) for mobility only, (c) NPIs and mobility. Mobility only was not *significantly* preferred by WAIC. Y axis are covariates and X axis the regression effect sizes

from that of estimating the effects of NPIs, preventing confounding within the transmission model, and can scale to many more regions. The second analysis uses both mobility and a lockdown indicator within a causal mediation analysis. This is intended to be a first step in the direction of accounting for causal relationships between variables that explain changes in transmission.

8.1 A Two-Stage Analysis

A two stage analysis (Haug et al., 2020) is one statistically principled way to estimate the (non causal) effect of NPIs and mobility without confounding within the transmission model. We first estimate R_t through the model via a daily random walk process which makes no prior assumptions about intervention/mobility mechanism or effectiveness. This random process can therefore select any arbitrary function of R_t that can best describe the data without any prior information about which interventions happened when or how well they worked. Given these estimates of R_t for all 11 European countries, we can run a simple partial pooling model to see if interventions and/or mobility can reproduce the trends in R_t. The model used is a linear regression with country level intercepts (to account for variation in R_0), and both joint and country specific effect sizes for interventions/mobility. As with the earlier analysis we use a hierarchical shrinkage prior on the coefficients (Piironen and Vehtari, 2017).

We run three versions of the model: NPIs only (NPI_only), mobility only (Mobility_only), and both NPIs and mobility (NPI+Mobility). MCMC convergence diagnostics in all cases did not indicate problems. We found the best fitting model to be NPI+Mobility. Relative to this model the expected log posterior difference ($\pm$ standard error) in WAIC of the model with only NPIs is -5.2 ± 4, ad -565.6 ± 49.2 with only mobility. Therefore, in fits to the estimated R_t, the model with mobility alone is substantially worse than the models with NPIs. The models with NPIs are not significantly different. This analysis could be improved using Bayesian leave-one-out cross-validation (Vehtari, Gelman, and Gabry, 2017) to account for the time series nature of the data. As in Flaxman et al. (2020b), the largest effect size is attributed to lockdown, as seen in Figure 1. This is true with and without the inclusion of the mobility variable.

A key advantage of this approach is that it is scalable to a large number of regions. R_t can be estimated in each region in parallel using separate models. Partial pooling can still be leveraged to estimate effects in the second stage. Once R_t has been estimated, any number of interesting statistical analyses can be conducted. A clear disadvantage is that effects are not fitted jointly with other epidemiological parameters, and it is therefore difficult to interpret how well the model fit to R_t extends to fitting the observed death data. Such an analysis may therefore be better at explaining trends in transmission, rather than the evolution of a disease across a country. Even so, this approach does not consider causal factors. This is the focus of the next example.

8.2 Causal Mediation

Here we perform a causal mediation analysis with just lockdown and mobility. Lockdown is used because it is the NPI with the largest effect size in both Section 8.1 and in Flaxman et al. (2020b), and because performing causal mediation with all NPIs in challenging.

We can hypothesise that changes in mobility are both an effect of lockdown and a cause of reductions in transmission.

Causal mediation analysis provides a means to disentangle the total effect of a lockdown into a direct and indirect effect. The indirect effect on changes in transmission occurs via some mediator, which in this case is hypothesised to be mobility. Further information about causal mediation can be found here (Pearl, 2009; Pearl, 2012). Briefly, to perform causal mediation we consider two transmission models

$$R^1_{t,m} = \tilde{R}^1_m \exp\left(\left(\beta^1_1 + \beta^1_{1,m}\right) L_{t,m} + \epsilon^1_{t,m}\right), \tag{13}$$

$$R^2_{t,m} = \tilde{R}^2_m \exp\left(\left(\beta^2_1 + \beta^2_{1,m}\right) L_{t,m} + \left(\beta^2_2 + \beta^2_{2,m}\right) M_{t,m} + \epsilon^2_{t,m}\right), \tag{14}$$

where $L_{t,m}$ is a binary indicator for lockdown and $M_{t,m}$ is mobility in country m respectively. $\tilde{R}^i_m$ and $\epsilon^i_{t,m}$ are country specific parameters modeling baseline transmission and a weekly random walk respectively. All other aspects of both models are the same as in (Flaxman et al., 2020b). Model (13) includes effects for lockdown, while (14) additionally considers mobility. β^1_1 is the total effect for lockdown, while β^2_1 is the partial effect when controlling for mobility. The mediated effect is therefore $\beta^1_1 - \beta^2_1$. This quantifies the effect of lockdown *via the path through mobility*. We find this mediated effect reduces R_t by 18.3% with a 95% credible interval of $[12.2\%, 44.4\%]$. The posterior probability of the effect being greater than 0 is 89.6% . Individual coefficients are shown in Figure 2.

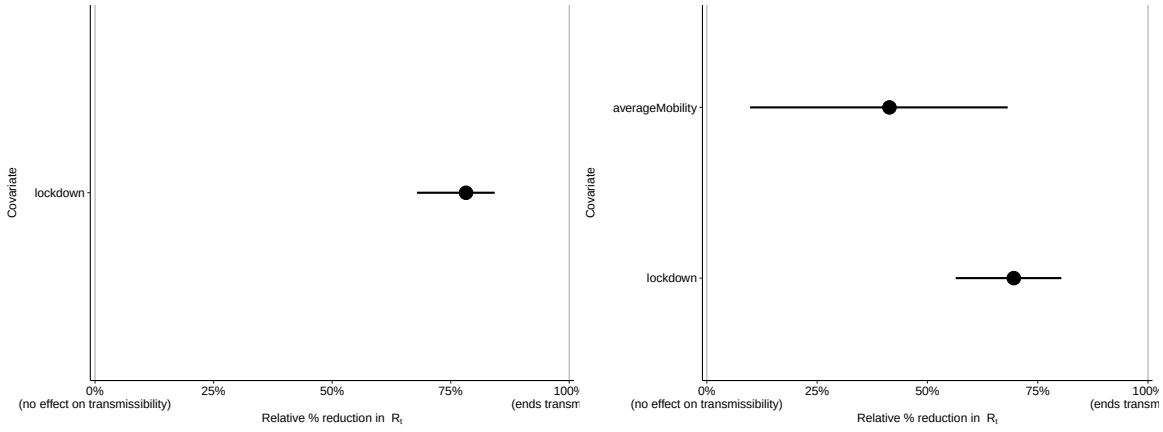

(a) (b)

Figure 2: Mediation analysis (a) Lockdown, (b) Lockdown and Mobility

These mediation results suggest a causal link between lockdown and mobility that eventually leads to reduced transmission rates. They also suggest that the mediated effect is far less than the total effect of lockdown, suggesting lockdown will have other causal pathways. Of course, mobility is also mediated through other pathways, and a principled causal analysis is out of the scope of this article. Nonetheless, this simple analysis with lockdown adds support to causal considerations.

9 Discussion

The model discussed in this article has appeared in various forms for specific analyses during the Covid-19 crisis. At the time of writing, it continues to be used to inform public policy. By presenting this model in a general form, we hope to stimulate discussion around it. A number of possible enhancements have not been discussed here. These include explicitly modeling importations, and allowing for uncertainty in the generation and infection to observation distributions. The Hamiltonian Monte Carlo sampler is used to fit the model, but can have difficulty converging when latent infections are modeled directly, or when regions are modeled jointly. We conjecture that convergence may be improved by carefully choosing initial parameters for the sampler. Future research could explore whether alternative samplers can be developed to fit these models more quickly.

A key difficulty within our framework is dealing with confounded variables, particularly those used to explain changes in transmission during the early stages of an epidemic. The analyses in Section 8 explore this issue, and contradict any

conclusion that complete lockdown has no or little effect. Rather, the analysis supports the central findings of Flaxman et al. (2020b): that lockdown and other NPIs served to control the first wave of the epidemic in 11 European countries.

References

Badr, Hamada S. et al. (2020). "Association between mobility patterns and COVID-19 transmission in the USA: a mathematical modelling study". In: *The Lancet Infectious Diseases*. ISSN: 14744457.

Bartoszynski, Robert (1967). "Branching Processes and the Theory of Epidemics". In: *Proceedings of the Fifth Berkeley Symposium on Mathematical Statistics and Probability*.

Bellman, R. and T. E. Harris (1948). "On the Theory of Age-Dependent Stochastic Branching Processes". In: *Proceedings of the National Academy of Sciences*. ISSN: 0027-8424.

Bellman, Richard and Theodore Harris (1952). "On Age-Dependent Binary Branching Processes". In: *The Annals of Mathematics*. ISSN: 0003486X.

Bettencourt, Luís M.A. and Ruy M. Ribeiro (2008). "Real time bayesian estimation of the epidemic potential of emerging infectious diseases". In: *PLoS ONE*. ISSN: 19326203.

Cauchemez, Simon et al. (2008). "Estimating the impact of school closure on influenza transmission from Sentinel data". In: *Nature*. ISSN: 14764687.

Champredon, David, Jonathan Dushoff, and David J.D. Earn (2018). "Equivalence of the Erlang-distributed SEIR epidemic model and the renewal equation". In: *SIAM Journal on Applied Mathematics*. ISSN: 00361399.

Cori, Anne et al. (2013). "A new framework and software to estimate time-varying reproduction numbers during epidemics". In: *American Journal of Epidemiology*. ISSN: 00029262.

Cowling, Benjamin J. et al. (2020). "Impact assessment of non-pharmaceutical interventions against coronavirus disease 2019 and influenza in Hong Kong: an observational study". In: *The Lancet Public Health*. ISSN: 24682667.

Ferguson, N. M., C. A. Donnelly, and R. M. Anderson (2001). "Transmission intensity and impact of control policies on the foot and mouth epidemic in Great Britain". In: *Nature*. ISSN: 00280836.

Flaxman, S et al. (Sept. 2020a). "Report 13: Estimating the number of infections and the impact of non-pharmaceutical interventions on COVID-19 in 11 European countries". In: *Stat. Comput.* in press.1, pp. 111–119.

Flaxman, Seth et al. (2020b). "Estimating the effects of non-pharmaceutical interventions on COVID-19 in Europe". In: *Nature*. ISSN: 1476-4687. URL: https://doi.org/10.1038/s41586-020-2405-7.

Fraser, Christophe (2007). "Estimating individual and household reproduction numbers in an emerging epidemic". In: *PLoS ONE*. ISSN: 19326203.

Fraser, Christophe et al. (2009). "Pandemic potential of a strain of influenza A (H1N1): Early findings". In: *Science*. ISSN: 00368075.

Gelman, Andrew and Jennifer Hill (2006). *Data Analysis Using Regression and Multilevel/Hierarchical Models*.

Getz, Wayne and James Lloyd-Smith (2006). "Basic methods for modeling the invasion and spread of contagious diseases". In.

Haug, Nils et al. (2020). "Ranking the effectiveness of worldwide COVID-19 government interventions". In: *MedRxiv*.

HKSAR, SARS Expert Committee of (2003). *Chronology of the SARS epidemic in Hong Kong*. Tech. rep. Hong Kong.

Hox, Joop J, Mirjam Moerbeek, and Rens de Schoot (2010). *Multilevel analysis: Techniques and applications*. Routledge.

Kelly, Heath A. et al. (2010). "Pandemic (H1N1) 2009 influenza community transmission was established in one Australian state when the virus was first identified in North America". In: *PLoS ONE*. ISSN: 19326203.

Kermack, William Ogilvy and McKendrick, A. G. (1927). "A contribution to the mathematical theory of epidemics". In: *Proceedings of the Royal Society of London. Series A, Containing Papers of a Mathematical and Physical Character*. ISSN: 0950-1207.

Kreft, Ita and Jan de Leeuw (2011). *Introducing Multilevel Modeling*.

Li, Ruiyun et al. (2020). "Substantial undocumented infection facilitates the rapid dissemination of novel coronavirus (SARS-CoV-2)". In: *Science*. ISSN: 10959203.

May, Robert M. (1976). "Simple mathematical models with very complicated dynamics". In: *Nature*. ISSN: 00280836.

Mellan, T A et al. (2020). *Report 21 - Estimating COVID-19 cases and reproduction number in Brazil*.

Miller, Andrew C et al. (2020). "Mobility trends provide a leading indicator of changes in SARS-CoV-2 transmission". In: *medRxiv*. URL: https://www.medrxiv.org/content/early/2020/05/11/2020.05.07.20094441.

Mishra, Swapnil et al. (2020). "A COVID-19 Model for Local Authorities of the United Kingdom". In: *medRxiv*. eprint: https://www.medrxiv.org/content/early/2020/11/27/2020.11.24.20236661.full.pdf. URL: https://www.medrxiv.org/content/early/2020/11/27/2020.11.24.20236661.

Nouvellet, Pierre et al. (2018). "A simple approach to measure transmissibility and forecast incidence". In: *Epidemics*. ISSN: 18780067.

NYS Press Office (2020). *Amid Ongoing COVID-19 Pandemic, Governor Cuomo Announces State is Bringing in International Experts to Help Advise the State's Reopening Plan*. URL: https://www.governor.ny.gov/news/amid-ongoing-covid-19-pandemic-governor-cuomo-announces-state-bringing-international-experts.

Olney, Andrew M et al. (2020). "Estimating the Effect of Social Distancing Interventions on COVID-19 in the United States". In: *medRxiv*.

Pearl, Judea (2009). "Causal inference in statistics: An overview". en. In: *Stat. Surv.* 3, pp. 96–146.

— (2012). "The causal mediation formula—a guide to the assessment of pathways and mechanisms". In: *Prev. Sci.* 13.4, pp. 426–436.

Piironen, Juho and Aki Vehtari (2017). "Sparsity information and regularization in the horseshoe and other shrinkage priors". en. In: *Electron. J. Stat.* 11.2, pp. 5018–5051.

Riley, Steven et al. (2003). "Transmission dynamics of the etiological agent of SARS in Hong Kong: Impact of public health interventions". In: *Science*. ISSN: 00368075.

The Scottish Government (2020). *Coronavirus (COVID-19): modelling the epidemic*. URL: https://www.gov.scot/collections/coronavirus-covid-19-modelling-the-epidemic/.

Thompson, W. A., Howard M. Taylor, and Samuel Karlin (1985). "An Introduction to Stochastic Modeling." In: *Journal of the American Statistical Association*. ISSN: 01621459.

Tokuda, Tomoki et al. (2011). "Visualizing distributions of covariance matrices". In: *Columbia Univ., New York, USA, Tech. Rep*, pp. 18–18.

Unwin, H Juliette T et al. (2020). "State-level tracking of COVID-19 in the United States". In: *Spirales*.

Vehtari, Aki, Andrew Gelman, and Jonah Gabry (Sept. 2017). "Practical Bayesian model evaluation using leave-one-out cross-validation and WAIC". In: *Stat. Comput.* 27.5, pp. 1413–1432.

Vollmer, Michaela A C et al. (2020). "A sub-national analysis of the rate of transmission of COVID-19 in Italy". In: *medRxiv*.

Wallinga, Jacco and Peter Teunis (2004). "Different epidemic curves for severe acute respiratory syndrome reveal similar impacts of control measures". In: *American Journal of Epidemiology*. ISSN: 00029262.

WHO (2003). *SARS: chronology of a serial killer.* Tech. rep.

10 Appendix

10.1 Offspring Dispersion

Define the offspring distribution of any given infection to be the distribution of the random number of offspring attributable to that infection. We show that assuming the variance of these distributions are a constant proportion of the mean implies, under suitable independence assumptions, the same result for new infections I_t for all time points.

Assume some ordering over infections at each period, and let $O_t^{(i)}$ denote the number of offspring of the i^{th} infection at time t. This can be decomposed as

$$O_t^{(i)} = \sum_{s=t+1}^{\infty} O_{ts}^{(i)}, \tag{15}$$

where $O_{ts}^{(i)}$ are the number of offspring of i birthed at time s. The branching process behind Equation (5) implies that $O_{ts}^{(i)}$ has mean $R_s g_{s-t}$. Assume that $\{O_{ts}^{(i)} : s \geq t\}$ are mutually independent and have variance which is a fixed proportion d of the mean. By Equation (15), this implies the same variance relationship for $O_t^{(i)}$. In particular, if $R_s = R_t$ for $s > t$ then $O_t^{(i)}$ has mean R_t and variance dR_t. New infections at time t can be expressed as

$$I_t = \sum_{s=1}^{t-1} \sum_{i=1}^{I_s} O_{st}^{(i)}. \tag{16}$$

Assume that all $O_{st}^{(i)}$ appearing in Equation (16) are mutually independent conditional on everything occurring up to time $t-1$, the result clearly follows by taking the variance of both sides of Equation 16 given R_t and $I_{v:t-1}$.

10.2 Population Adjustment

Here we motivate Equation (7), which is used to adjust transmission rates for the size of the infectable population. The most obvious starting point for such an adjustment would be to let

$$\mathrm{E}[I_t | R_t, I_{v:t-1}] = \left(\frac{S_0 - I_{t-1}}{S_0} \right) R_{u,t} L_t, \tag{17}$$

where R_{u_t} is defined as in Section 4.2. This is similar in form to a *discrete logistic growth model*. Such models are well known as examples of simple models that exhibit chaotic dynamics (May, 1976). In particular, it is possible that the expected value on the left hand side exceeds the remaining susceptible population. Intuitively, this issue occurs because multiple infections can occur simultaneously in the discrete model. We therefore propose solving this by using a population adjustment motivated by the solution to a continuous time model whose intensity is a simplification of Equation (3).

Suppose we observe $I_{v:t-1}$ and current transmission R_t. We evolve infections from time $t-1$ to t continuously, and hence avoid overshooting. Define a continuous time counting $\tilde{I}(s)$ process starting at time $t-1$ by the intensity

$$\tilde{\lambda}(s) = \left(\frac{S_0 - \tilde{I}(s)}{S_0} \right) R_{u,t} L_t, \tag{18}$$

for $s \geq t-1$, and with initial condition $\tilde{I}(t-1) = I_{t-1}$. Supplementary 11.1 shows that

$$\mathrm{E}[\tilde{I}(t)] = I_{t-1} + (S_0 - I_{t-1}) \left(1 - \exp\left(-\frac{R_{u,t} L_t}{S_0} \right) \right), \tag{19}$$

which is the motivation for Equation (7).

11 Online Supplement

11.1 Proof of Equation (19)

Without loss of generality, we prove the result for time $t = 1$. The argument remains the same for all $t > 1$.

From Thompson, Taylor, and Karlin, 1985, Lemma 5.5, we have

$$\mathrm{E}[\tilde{I}(s)] = \tilde{I}(0) + \int_0^s \mathrm{E}[\tilde{\lambda}(l)]dl \text{ for } s \geq 0.$$

The following lemma derives an expression for the the expected intensity on the right hand side.

Lemma 11.1. *The expected intensity takes the form*

$$E[\tilde{\lambda}(s)] = \tilde{\lambda}(0) \exp\left(-\frac{R_{u,1}L_1}{S_0}s\right),$$

for all $s \geq 0$.

Proof of Lemma 11.1. Fix $s \geq 0$, some small $\Delta > 0$ and let $h(s) := \mathrm{E}[\tilde{\lambda}(s)]$. We have from Equation (18) that

$$h(s+\Delta) = \left(\frac{S_0 - \mathrm{E}[\tilde{I}(s+\Delta)]}{S_0}\right) R_{u,1}L_1. \tag{20}$$

We can write

$$\mathrm{E}[\tilde{I}(s+\Delta)|\tilde{\lambda}(s)] = \mathrm{E}[\tilde{I}(s)|\tilde{\lambda}(s)] + \tilde{\lambda}(s)\Delta + \mathcal{O}(\Delta),$$

and taking expectations on both sides,

$$\mathrm{E}[\tilde{I}(s+\Delta)] = \mathrm{E}[\tilde{I}(s)] + h(s)\Delta + \mathcal{O}(\Delta).$$

Substituting this into (20) and rearranging gives

$$\begin{aligned} h(s+\Delta) &= \left(\frac{S_0 - \mathrm{E}[\tilde{I}(s+\Delta)]}{S_0}\right) R_{u,1}L_1 - \frac{R_{u,1}L_1}{S_0}\left(h(s)\Delta + \mathcal{O}(\Delta)\right), \\ &= h(s) - \frac{R_{u,1}L_1}{S_0}\left(h(s)\Delta + \mathcal{O}(\Delta)\right). \end{aligned}$$

Rearranging gives

$$\frac{h(s+\Delta) - h(s)}{\Delta} = -\frac{R_{u,1}L_1}{S_0}\left(h(s) + \frac{\mathcal{O}(\Delta)}{\Delta}\right).$$

Taking the limit as $\Delta \to 0$ and rearranging gives the differential equation

$$\frac{h'(s)}{h(s)} = -\frac{R_{u,1}L_1}{S_0}.$$

Integrating both sides gives

$$\log(h(s)) = -\frac{R_{u,1}L_1}{S_0}s + C.$$

Using that $h(0) = \tilde{\lambda}(0)$ gives the constant $C = \log(\tilde{\lambda}(0))$. Plugging in yields the required result. □

Hence,

$$\begin{aligned}
\mathrm{E}[\tilde{I}(s)] &= I_0 + \tilde{\lambda}(0) \int_0^s \exp\left(-\frac{R_{u,1}L_1}{S_0} l\right) dl \\
&= I_0 + \tilde{\lambda}(0) \frac{S_0}{R_{u,1}L_1} \left(1 - \exp\left(-\frac{R_{u,1}L_1}{S_0} s\right)\right) \\
&= I_0 + (S_0 - \tilde{I}(s)) \left(1 - \exp\left(-\frac{R_{u,1}L_1}{S_0} s\right)\right).
\end{aligned}$$

Letting $s = 1$ gives the required result.